J. Am. Chem. Soc. **1982**, *104*, 4803–4810

lowing terms. In aqueous solution (at 4×10^{-5} M probe concentration), only unimolecular emission (monomer and excimer) is observed. The addition of very low levels of polyion (7.3×10^{-6} M) results in substantial extraction of the probe from the aqueous domain to that of the polyion. Both intermolecular and intramolecular excimer formations are enhanced, and the contribution of probe emission from the aqueous phase is significantly decreased. Eventually, at $\sim 5 \times 10^{-5}$ M polyion concentration, the fluorescence intensity maximizes. Further addition of polyion causes separation of probe molecules over the larger number of available sites, and the intermolecular component decreases, allowing the monomer emission to become more pronounced.

Summary

The excimer emissions of NDNP and NMA are dramatically enhanced in the presence of polyelectrolyte (NaPSS) in aqueous solution. This enhancement is attributed to the association (due to hydrophilic, electrostatic, and hydrophobic interactions) of the probes with microanions. The intermolecular excimer formation rate constant, k_1, of NMA is enhanced by 10^3 in the presence of 8×10^{-5} M NaPSS. Both intramolecular and intermolecular excimer formation of NDNP occur in the presence of NaPSS in aqueous solution. NaCl and $Co(NH_3)_5Cl_3$ retard excimer formation, while high pressure increases both the emission intensity and the lifetime of the excimer of NDNP.

Acknowledgment. We thank the National Science Foundation for its generous support of this work. We also thank Professor H. Morawetz for informative and helpful comments concerning his previous related investigations and interpretations.

Registry No. NDNP, 17018-62-1; NaPSS, 25704-18-1; NMA, 39110-74-2.

Photochemistry of $Ru(bpy)_3^{2+}$

Bill Durham,[1] Jonathan V. Caspar, Jeffrey K. Nagle, and Thomas J. Meyer*

Contribution from the Department of Chemistry, The University of North Carolina, Chapel Hill, North Carolina 27514.
Received December 4, 1980.
Revised Manuscript Received March 1, 1982

Abstract: Temperature-dependent lifetime data in dichloromethane are reported for the emitting charge-transfer excited state of $Ru(bpy)_3^{2+}$ (^{3}CT) (bpy is 2,2′-bipyridine) under photochemical (NCS^- salt) and nonphotochemical (PF_6^- salt) conditions. Temperature-dependent lifetime data have also been obtained in dichloromethane for the salts $[Ru(bpy)_2(py)_2](PF_6)_2$ (py is pyridine) and $[Ru(phen)_3](PF_6)_2$ (phen is 1,10-phenanthroline) as have temperature-dependent quantum-yield data for photochemical loss of bpy, $[Ru(bpy)_3]X_2\ (+h\nu) \rightarrow [(bpy)_2RuX(bpy)]X \rightarrow (bpy)_2RuX_2 + bpy$, for the salt $[Ru(bpy)_3](NCS)_2$ ($\phi_p(25\ °C) = 0.068$). The data obtained here, combined with the data and suggestions made earlier by Van Houten and Watts (ref 2 and 11) based on their experiments in water, suggest a detailed view of the microscopic events which lead to photosubstitution. Initial excitation leads to a charge-transfer state largely triplet in character, ^{3}CT. The CT state undergoes thermal activation to give a d–d excited state. The d–d state undergoes further thermal activation by loss of a pyridyl group to give a five-coordinate intermediate which is apparently square pyramidal in structure. The fate of the intermediate is capture of a sixth ligand, either by solvent or an anion held close to the activated metal center by ion-pairing or by chelate ring closure to return to $Ru(bpy)_3^{2+}$. Capture by solvent or an anion leads to a six-coordinate, unidentate bpy intermediate $(bpy)_2(L)Ru^{II}(py\text{–}py)$ which can either undergo chelate ring closure and loss of L to return to $Ru(bpy)_3^{2+}$ or loss of bpy to give photoproducts. At room temperature and above, $Ru(bpy)_3^{2+}$ is in an intrinsic sense relatively reactive photochemically in either dichloromethane or water. The apparent solvent effect between dichloromethane and water may arise largely from the thermodynamic and/or kinetic preferences of the six-coordinate unidentate bpy intermediate and not in steps involving excited states. The apparent photochemical stability of $Ru(bpy)_3^{2+}$ in water is a consequence of the dominance of chelate ring closure and not of an inherently low photochemical reactivity.

Introduction

Although the excited-state properties of $Ru(bpy)_3^{2+}$ (bpy is 2,2′-bipyridine) have been studied in detail[2–7] and the excited state(s) have provided the basis for a number of interesting applications,[8,9] the photochemical properties of this and related complexes have been largely neglected. The photochemical decomposition of $Ru(bpy)_3^{2+}$ in water[10,11] and DMF[12,13] has been studied, and a marked enhancement in quantum yield has been noted in dichloromethane.[14] In related complexes, photochemical substitution in *cis*-$Ru(bpy)_2(py)_2^{2+}$ (py is pyridine) has been shown to be of synthetic value[15] and both photochemical cis $\rightleftharpoons$ trans isomerization and ClO_4^- oxidation have been observed for $Ru(bpy)_2(H_2O)_2^{2+}$.[16]

We report here the results of detailed photochemical and photophysical studies on $Ru(bpy)_3^{2+}$ and the related complexes $Ru(phen)_3^{2+}$ (phen is 1,10-phenanthroline) and $Ru(bpy)_2(py)_2^{2+}$ in dichloromethane solution. When combined with the earlier results of Van Houten and Watts,[10,11] a detailed picture begins to emerge of the mechanistic and excited-state properties which lead to the observed photochemistry.

---

(1) Department of Chemistry, University of Chemistry, University of Arkansas, Fayetteville, Ark. 72701.

(2) Van Houten, J.; Watts, R. J. *J. Am. Chem. Soc.* **1975**, *97*, 3843.

(3) Balzani, V.; Moggi, L.; Manfrin, M. F.; Bolletta, F.; Laurence, G. S. *Coord. Chem. Rev.* **1975**, *15*, 321.

(4) Hager, G. D.; Crosby, G. A. *J. Am. Chem. Soc.* **1975**, *97*, 7031. Hipps, K. W.; Crosby, G. A. *Ibid.* **1975**, *97*, 7042.

(5) Meisel, D.; Matheson, M. S.; Mulac, W. A.; Rabani, J. *J. Phys. Chem.* **1977**, *81*, 1449.

(6) Creutz, C.; Sutin, N. *Proc. Natl. Acad. Sci. U.S.* **1975**, *72*, 2858.

(7) Felix, F.; Ferguson, J.; Güdel, H. U.; Ludi, A. *J. Am. Chem. Soc.* **1980**, *102*, 4096.

(8) (a) Balzani, V.; Bolletta. F.; Gandolfi, M. T.; Maestri, M. *Top. Curr. Chem.* **1978**, *75*, 1. (b) Meyer, T. J. *Isr. J. Chem.* **1977**, *15*, 200.

(9) (a) Meyer, T. J. *Acc. Chem. Res.* **1978**, *11*, 94. (b) Sutin, N. *J. Photochem.* **1979**, *10*, 19.

(10) Van Houten, J.; Watts, R. J. *J. Am. Chem. Soc.* **1976**, *98*, 4853.

(11) Van Houten, J.; Watts, R. J. *Inorg. Chem.* **1978**, *17*, 3381.

(12) Hoggard, P. E.; Porter, G. B. *J. Am. Chem. Soc.* **1978**, *100*, 1457.

(13) Wallace, W. M.; Hoggard, P. E. *Inorg. Chem.* **1979**, *18*, 2934.

(14) Gleria, M.; Minto, F.; Beggiato, G.; Bortolus, P. *J. Chem. Soc., Chem. Commun.* **1978**, 285.

(15) Durham, B.; Walsh, J. L.; Carter, C. L.; Meyer, T. J. *Inorg. Chem.* **1980**, *19*, 860.

(16) Durham, B.; Wilson, S. R.; Hodgson, D. J.; Meyer, T. J. *J. Am. Chem. Soc.* **1980**, *102*, 600.

0002-7863/82/1504-4803$01.25/0

Experimental Section

Materials. $[Ru(bpy)_3](SCN)_2$ was prepared as described by Hoggard and Porter.[12] $[Ru(phen)_3](SCN)_2$ (phen is 1,10-phenanthroline) and $[Ru(bpy)_3]Br_2$ were prepared in an analogous manner. Dichloromethane was reagent grade and used without further purification except in the experiments where noted. In those cases the solvent was purified by washing approximately 4 L with 10–20 mL of concentrated sulfuric acid, once with dilute KOH, followed by several washings with water. The dichloromethane was dried overnight over $MgSO_4$ and finally distilled.

Equipment. UV–visible spectra were obtained using a Bausch and Lomb Spectronic 210UV spectrophotometer. Fluorescence spectra were obtained using a Hitachi Perkin-Elmer fluorescence spectrophotometer, Model MPF-2A. The spectra were uncorrected.

Photochemical Procedures. Quantum yield measurements and other investigative photolyses were carried out using radiation from a Hanovia 97730010 1000-W Hg-Xe arc lamp in a LH151N Schoeffel lamp housing and passed through a Bausch and Lomb monochromator (No. 33-66-79). With a 6-mm entrance and 1-mm exit slit width, the predicted bandwidth is less than 10 nm. The sample solutions were contained in 1-cm² fluorescence cells which in turn were held in an aluminum cell holder which was drilled out to allow water from a large temperature bath to circulate through. A thermistor, Omega Engineering No. H-106-UUA35J3, attached to the aluminum cell holder, was used to measure the temperature. Samples were allowed to equilibrate for a minimum of 30 min before irradiation. For low-temperature measurements a low positive pressure of dry nitrogen was maintained in the box which housed the cell holder and associated optics to prevent fogging. The sample solutions were either air saturated or freeze–pump–thaw degassed (4 cycles). Above 35 °C the sample solutions were sealed in Pyrex test tubes. The intensity of the incident radiation in these cases was determined by comparing runs made in Pyrex tubes at lower temperatures with those made in the usual fluorescence cells at the same temperatures.

Quantum yields were determined by monitoring the decay of the characteristic $Ru(bpy)_3^{2+*}$ luminescence as a function of time. The emitted light was collected with a simple convex lens and passed through a Corning 3-70 cutoff filter; the intensity was measured with a RCA1P28A photomultiplier tube mounted at right angles to the incident beam. The output was recorded on a Hewlett-Packard 7004B X–Y recorder. The initial concentration of reactant was maintained such that the absorbances of the solutions were less than 0.4, in which case a linear dependence of the intensity of the emitted light vs. concentration was followed.[17] The proportionality constant for the conversion of emission intensity back to concentration was obtained from the initial intensity measurement. Actinometry on the incident beam was performed using Reinecke's salt in the same cell and under similar conditions as above and was treated according to the method described by Adamson.[18]

The emission intensity was converted into concentration of $Ru(bpy)_3^{2+}$ which was in turn used in the equations below to calculate quantum yields.

$$R_t = ([A]_t - [A]_{t+\Delta t})/\Delta t$$

R_t is the slope of the concentration vs. time curve at time t. At $t = 0$, this slope exactly gives the quantum yield, ϕ, for the process

$$A \xrightarrow{h\nu} B$$

By definition

$$-d[A]/dt = I_a\phi = R_t$$

I_a is the "light" intensity absorbed by species A, given by

$$I_a = I_0(1 - 10^{-\epsilon_A l[A]})$$

where ϵ_A is the extinction coefficient of species A at the irradiation wavelength and l is the path length (all data were collected in 1-cm cells, and hence l will be deleted from here on). At times after $t = 0$, a portion of the incident light will be absorbed by product (B) molecules; hence the quantum yield at any time, t, is given by

$$\phi = kR_t/\epsilon_A[A]_t I_0(1 - 10^{-k}) \qquad (1)$$

where

$$k = (\epsilon_A - \epsilon_B)[A]_t + \epsilon_B[A]_0$$

The value of k is the total solution absorbance at any time; ϵ_B is the extinction coefficient of B at the irradiation wavelength and $[A]_0$ is the initial concentration of the photoactive species. The term $I_0(1 - 10^{-k})$ in the quantum yield expression gives the total intensity of absorbed light at any time, and the term $k/\epsilon_A[A]_t$ simply corrects for the light absorbed by the photoinert product molecules.

The following extinction coefficients at 436 nm were used: $Ru(bpy)_3^{2+}$, 12000; $Ru(bpy)_2Cl_2$, 4050; $Ru(bpy)_2Br_2$, 4050; $Ru(bpy)_2(NCS)_2$, 4000; $Ru(phen)_3^{2+}$, 6575. The calculations were not a sensitive function of the set of extinction coefficients used. The treatment was derived for the simple case A → B where both species absorb. No attempt was made to correct for the small concentration of monodendate bipyridine complexes which were present in some of the photolyses since the correction appears to be negligible. The yield was calculated for each time interval, Δt, and then averaged. The time interval could be varied to as short a period as desired since a continuous plot of emission intensity vs. time was available. Typically the time interval was chosen to allow 20 determinations within the time span for the emission intensity to fall by 75%. The quantum yields calculated for each interval showed only random departures from the mean for all times during a particular photolysis. The quantum yields determined in this manner were in excellent agreement with those determined from initial slopes of concentration vs. time plots but had the advantage of using a much larger percentage of the data. The reported errors are the standard deviations for the set of individual runs performed at each temperature. All of the above calculations were carried out on a PET Commodore microcomputer.

Lifetime Measurements. Lifetime measurements were obtained using a Molectron UV-400 nitrogen laser as a pulsed light source. The sample cell was constructed of Pyrex and consisted of two concentric cylinders. The inner cylinder which held the sample solution had two short arms at right angles to each other which projected through the outer cylinder and were fitted with flat windows. The outer cylinder was provided with inlet and outlet tubes and functioned as a water jacket. The temperature was regulated and monitored as described in the previous section. The inner tube also extended beyond the water jacket and was connected to a small round-bottom flask in which the sample solution could be placed during freeze–pump–thaw degassing. The solutions were cycled five or six times before sealing under vacuum. At right angles to the incident beam, the emitted radiation was monitored by an EMI9785B photomultiplier tube which was preceded by a monochromator (BL No. 33-66-79), a Corning 3-70 filter, and 2 cm of nitromethane to absorb scattered light from the laser. The output of the photomultiplier was fed to a Tektronix Model R 7912 transient digitizer and then into a Digital PDP 11/34 minicomputer. The lifetimes were determined by a weighted least-squares fit to a simple exponential decay. Lifetimes below 0 °C were measured using a dewar system with a quartz fluorescence cell. At the same temperature both setups gave identical results for measured lifetimes.

The emission efficiency measurements were made by comparing the emission of a solution of $[Ru(bpy)_3](PF_6)_2$ in water with that of a dichloromethane solution having the same absorbance. The experiment was performed with different combinations of cells, and nearly identical results were obtained. The solutions were held in fluorescence cells which were attached to 25-mL round-bottom flasks, freeze–pump–thaw degassed five times, and sealed under vacuum. Emission measurements were made using the same experimental approach as described for the quantum yield determinations including temperature control.

Results

Spectra. The visible absorption spectra of $Ru(bpy)_3^{2+}$ in 1 N H_2SO_4 and in CH_2Cl_2 are shown in Figure 1. Little or no difference is observed between the two media if the PF_6^- salt is the origin of $Ru(bpy)_3^{2+}$. With the NCS^- salt, however, there are some small differences in the low-energy ultraviolet spectral region in dichloromethane which may be due to the effect of ion pairing on intramolecular transitions. The low-energy CT (charge transfer) band usually observed at 453 nm is also shifted very slightly to 454 nm.

The emission maxima for $Ru(bpy)_3^{2+}$ with a variety of counterions in dichloromethane as well as values in H_2O and CH_3CN are given in Table I. The emission spectra, which are uncorrected, were obtained at room temperature in nitrogen or argon degassed solutions. The bands are reasonably broad, but the peak maxima are clearly distinguishable. Except for the tetraphenylborate anion, only very slight shifts in emission maxima were observed for the series of anions in dichloromethane.

Lifetimes. Excited-state lifetimes were measured as a function of temperature by luminescence decay measurements following laser flash photolysis at 337 nm. Lifetime data for $Ru(bpy)_3^{2+}$ at 25 °C in a variety of media are given in Table I. Tempera-

---

[17] Durham, B., unpublished results.

[18] Wegner, E. E.; Adamson, A. W. *J. Am. Chem. Soc.* **1966**, *88*, 394.

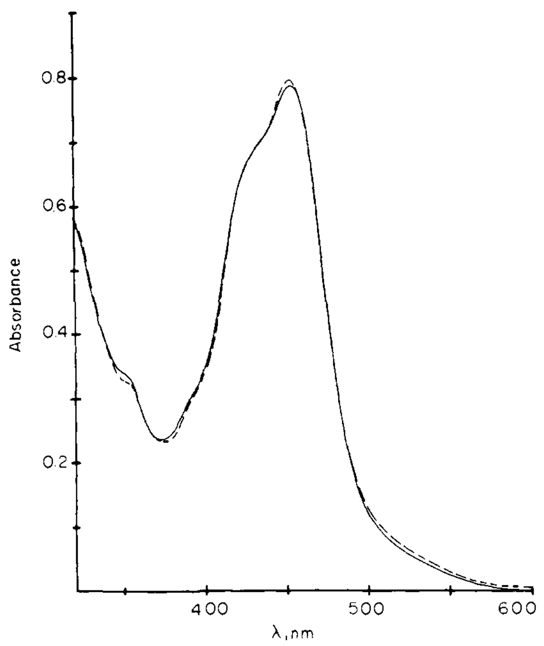

Figure 1. Visible spectra of [Ru(bpy)$_3$](PF$_6$)$_2$ in 1 N H_2SO_4 (---) and in CH_2Cl_2 (—).

Table I. Luminescence Maxima and Excited-State Lifetimes under Various Conditions for Ru(bpy)$_3^{2+}$ at 25 °C

counterion[a]	solvent	λ_{max}, nm[b]	τ_0, μs[c]
PF_6^-	CH_2Cl_2	597	0.68 (2)
ClO_4^-	CH_2Cl_2	598	0.75 (2)
SCN^-	CH_2Cl_2	598	0.69 (2)
$B(C_6H_5)_4^-$	CH_2Cl_2	592	
PF_6^-	H_2O	605	0.58 (2)
PF_6^-	CH_3CN	605	0.86 (2)

[a] Added as the counterion in salts containing Ru(bpy)$_3^{2+}$. [b] Uncorrected. [c] Measured emission lifetimes following excitation at 337 nm using laser flash photolysis.

ture-dependent lifetime data for Ru(bpy)$_3^{2+}$, Ru(phen)$_3^{2+}$, and Ru(bpy)$_2$(py)$_2^{2+}$ in CH_2Cl_2 under nonphotochemical conditions were obtained using PF_6^- as the counterion. In all three cases, the temperature dependence of the lifetime, $\tau(T)$, could be satisfactorily accounted for by assuming the relationship in eq 2

$$\tau(T)^{-1} = k + k'^0 \exp[-\Delta E'/RT] = k + k' \qquad (2)$$

suggested by Van Houten and Watts.[2,10,11] In eq 2, k is actually a composite rate constant which includes both radiative (k_r) and nonradiative (k_{nr}) contributions to the rate of excited-state decay from the lowest CT state or states (eq 3). It follows that the

$$k = k_r + k_{nr} \qquad (3)$$

quantum efficiency for emission, $\phi_r(T)$, is given by eq 4.

$$\phi_r(T) = k_r\tau(T) \qquad (4)$$

In their work on the excited-state decay of Ru(bpy)$_3^{2+*}$ in a series of solvents, Allsopp et al. find a better fit of their data at low temperatures to a more complicated expression which adds a second exponential term, $\exp(-\Delta E/RT)$, to account for a temperature dependence of k_{nr}.[19] From their treatment, $\Delta E << \Delta E'$. Our data were obtained at temperatures sufficiently high that the exponential term including ΔE can be neglected and the inclusion of a second exponential term did not noticeably improve our fits.

Temperature-dependent lifetime data were also obtained for Ru(bpy)$_3^{2+}$ in CH_2Cl_2 under photochemical conditions using the NCS^- salt. These data could also be fit to an equation of the form of eq 2. In figure 2 are shown plots of ln $\tau(T)$ vs. $1/T$ in CH_2Cl_2 for [Ru(bpy)$_3$](PF$_6$)$_2$, [Ru(bpy)$_2$(py)$_2$](PF$_6$)$_2$, and [Ru(bpy)$_3$](NCS)$_2$. In Table II the kinetic parameters obtained by fit of the data to eq 2 are given for the three complexes.

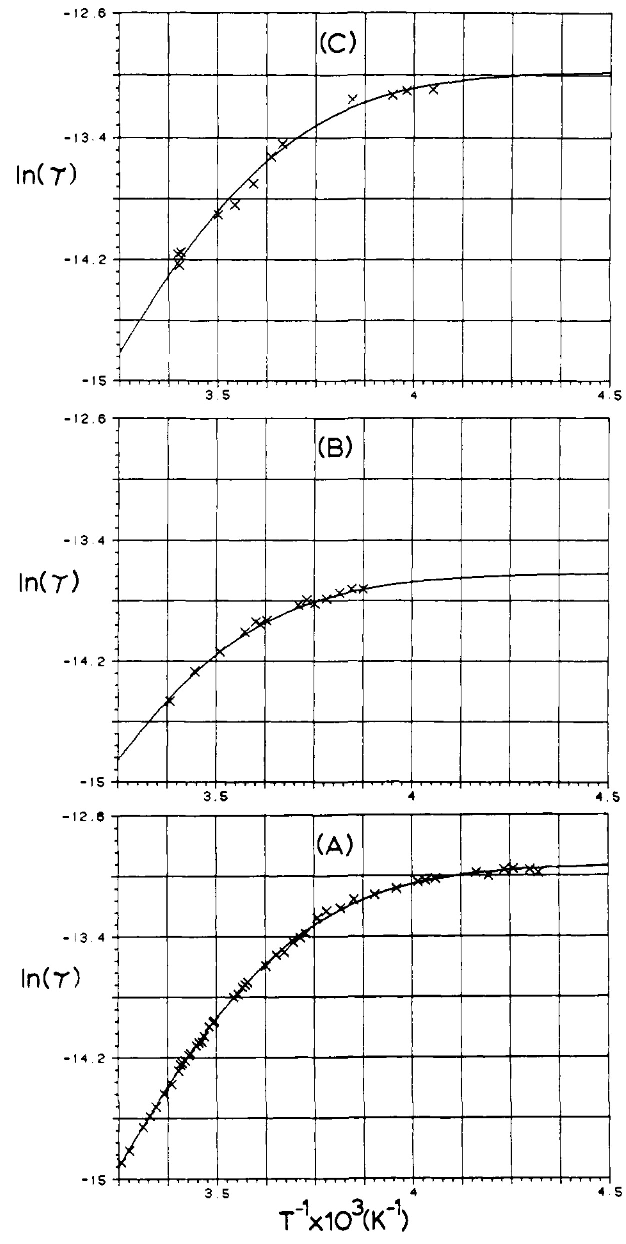

Figure 2. Comparison of experimental data with a computer-generated fit (note eq 2) of the temperature dependence for the emission lifetimes in CH_2Cl_2 of (A) [Ru(bpy)$_3$](PF$_6$)$_2$, (B) [Ru(bpy)$_2$(py)$_2$](PF$_6$)$_2$, and (C) [Ru(bpy)$_3$](NCS)$_2$.

Table II. Kinetic Data for Excited-State Decay Obtained by Temperature-Dependent Emission Measurements (Note Eq 2 and 3)

salt	solvent	$\Delta E'$, cm^{-1}	$10^{-5}k$, s^{-1}	10^{-13}-k'^0, s^{-1}
[Ru(bpy)$_3$](PF$_6$)$_2$	CH_2Cl_2	3563	4.11	4.5
	($k_r = 1.04 \times 10^5$ s^{-1}; $k_{nr} = 0.34 \times 10^6$ s^{-1})[a]			
Ru(bpy)$_3^{2+}$[b]	H_2O	3560	12.90	1.0
	($k_r = 0.69 \times 10^5$ s^{-1}; $k_{nr} = 1.22 \times 10^6$ s^{-1})[b]			
[Ru(bpy)$_3$](NCS)$_2$	CH_2Cl_2	3520	4.30	3.2
[Ru(bpy)$_2$(py)$_2$](PF$_6$)$_2$	CH_2Cl_2	3410	8.20	1.7
[Ru(phen)$_3$](PF$_6$)$_2$	CH_2Cl_2	3185	1.40	3.1

[a] $k = k_r + k_{nr}$; note eq 3. [b] From ref 10.

Where sufficient data were taken for [Ru(bpy)$_3$](PF$_6$)$_2$ and [Ru(phen)$_3$](PF$_6$)$_2$, kinetic parameters were obtained by a non-

---

(19) Allsopp, S. R.; Cox, A.; Kemp, T. J.; Reed, W. J. *J. Chem. Soc. Faraday Trans.* **1978**, *5*, 1275.

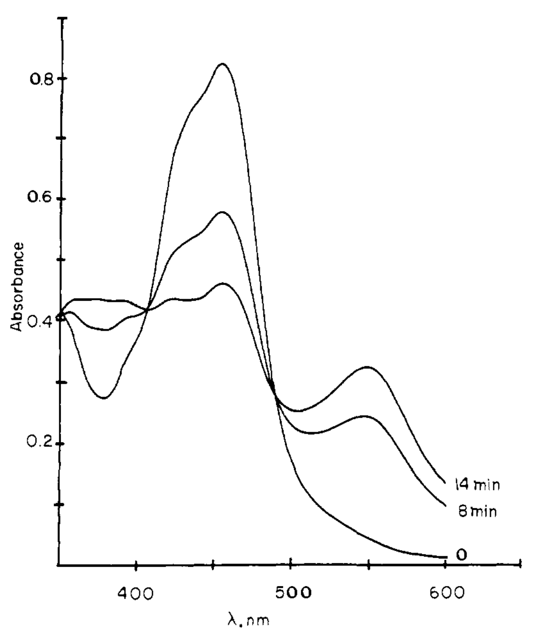

Figure 3. Visible spectra taken at various intervals during the photolysis of $[Ru(bpy)_3](Br_2)_2$ in CH_2Cl_2 at 25 °C.

linear least-squares procedure utilizing the Gauss–Newton algorithm. For the remaining cases, an iterative linear least-squares procedure was adopted. Good agreement was obtained between the two procedures and as shown by the plots in Figure 2, the agreement with the experimental data is excellent in all cases. Our kinetic parameters are in good agreement with those obtained by Van Houten and Watts in water[11] but do disagree somewhat with those reported by Allsopp et al.[19]

In order to obtain a more detailed comparison between excited-state properties in water and dichloromethane, the emission quantum yield in the latter solvent was determined at 25 °C. With $\phi_r(T)$ available, values of k_r and k_{nr} can be calculated (note eq 2–4), and the resulting values in the two solvents are also given in Table II.

The striking feature about the data in Table II is the near constancy in the kinetic parameters which describe excited-state decay for different solvents, under photochemical (NCS^- salt in CH_2Cl_2) and nonphotochemical (PF_6^- salt in CH_2Cl_2) conditions, and even between different complexes ($[Ru(bpy)_3](PF_6)_2$ compared to $[Ru(bpy)_2(py)_2](PF_6)_2$).

Photochemistry. As indicated by Gleria et al. for $[Ru(bpy)_3]Cl_2$,[14] we find that the net photochemistry of $Ru(bpy)_3^{2+}$ in the presence of a series of anions (Cl^-, Br^-, NCS^-) is well behaved. For the bromide salt, the spectral changes which occur during photolysis (Figure 3) are consistent with the net reaction

$$[Ru(bpy)_3]Br_2 \xrightarrow[CH_2Cl_2]{h\nu} Ru(bpy)_2Br_2 \qquad (5)$$

For $Ru(bpy)_2Br_2$ in CH_2Cl_2, λ_{max} = 548 nm (ϵ 9300) and λ_{max} = 378 nm (ϵ 9500). For the NCS^- salt, there is clear evidence that the loss of a 2,2′-bipyridine ligand occurs in a stepwise manner, since spectral evidence has been obtained for the monodentate intermediate, $[(bpy)_2Ru(NCS)bpy]^+$.[15] The monodentate intermediate is unstable and within minutes at room temperature in CH_2Cl_2 reacts further with NCS^- to give $Ru(bpy)_2(NCS)_2$. The overall photochemical mechanism in CH_2Cl_2 is then

$$[Ru(bpy)_3]X_2 \xrightarrow{h\nu} [(bpy)_2Ru(X)bpy]X \qquad (6)$$

$$[(bpy)_2RuX(bpy)]X \rightarrow Ru(bpy)_2X_2 + bpy \qquad (7)$$

We have determined quantum yield values for the first step (eq 6) by observing the loss in luminescence intensity in solutions of $[Ru(bpy)_3]X_2$ in CH_2Cl_2. The analysis should be specific for the first step since neither of the complexes $[Ru(bpy)_2(py)X]^+$ or $[(bpy)_2Ru(NCS)bpy]^+$ emits appreciably under the conditions of the quantum yield experiments. Given the low dielectric constant for CH_2Cl_2 (D_s = 8.9) and the available evidence, salts of $Ru(bpy)_3^{2+}$ in CH_2Cl_2 are essentially completely ion-paired in the medium as suggested by eq 6 and 7.

Table III. Photochemical Quantum Yields in CH_2Cl_2 at 25 °C in Aerated and Degassed Solutions

salt	$\phi_p(O_2)$ aerated	ϕ_p degassed
$[Ru(bpy)_3](NCS)_2$	0.039	0.068
$[Ru(bpy)_3]Cl_2$	0.062	0.100
$[Ru(bpy)_3]Br_2$	0.026	
$[Ru(phen)_3](NCS)_2$	0.010	0.020
$[Ru(phen)_3]Cl_2$	0.0086	0.014

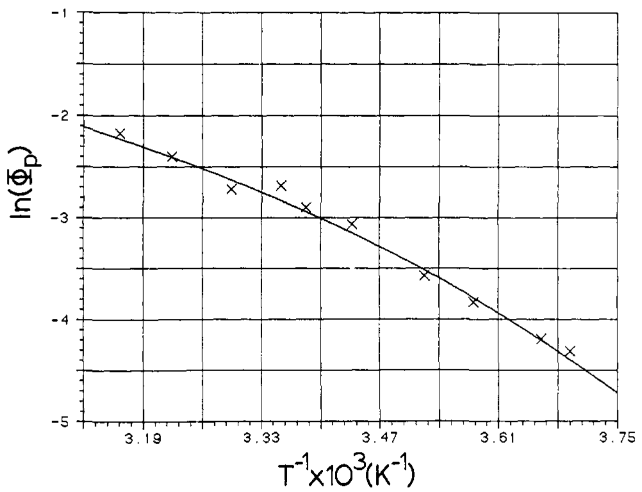

Figure 4. Temperature dependence of the quantum yield for the reaction between $Ru(bpy)_3^{2+}$ and thiocyanate ion in CH_2Cl_2. Experimental values are shown as crosses. The line through the data was calculated using eq 8, the appropriate lifetime data shown in Figure 2C, and the parameters, a/b = 667 and $\Delta E''$ = 1870 cm^{-1}.

Quantum yield data at 25 °C obtained in aerated and freeze–pump–thaw degassed solutions are summarized in Table III. The temperature dependence of the photochemical quantum yield, $\phi_p(T)$, for the salt $[Ru(bpy)_3](NCS)_2$ was also studied, and the data are presented in Figure 4 as a plot of ln $\phi_p(T)$ vs. $1/T$. Attempts were made to fit the data to the expressions in eq 8 and 9. In order to obtain a reasonable fit it was necessary to use eq

$$\phi_p = \left[\frac{k^0 \exp(-\Delta E'/RT)}{k + k^0 \exp(-\Delta E'/RT)}\right][a' \exp(-\Delta E''/RT)] \qquad (8)$$

$$\phi_p = \left[\frac{k^0 \exp(-\Delta E'/RT)}{k + k^0 \exp(-\Delta E'/RT)}\right]\left[\frac{a \exp(-\Delta E''/RT)}{b + a \exp(-\Delta E''/RT)}\right] \qquad (9)$$

9. The line in Figure 4 was drawn using an iterative least-squares approach. Values for k, k^0, and $\Delta E'$ were taken from the lifetime data in Table II, and the least-squares fitting routine gave, for the unknown constants in eq 8 and 9, a/b = 667 and $\Delta E''$ = 1870 cm^{-1}. The fitting procedure was based on 10 data points, and although there is a considerable uncertainty in the value of a/b, $\Delta E''$ does appear to be well defined.

Discussion

Excited States. The absorption and emission spectra of $Ru(bpy)_3^{2+}$ have been interpreted using a charge-transfer model.[4,7] The absorption spectrum is dominated by transitions to CT states largely singlet in character and to their vibronic components. At lower energies, much weaker bands are observed which are assignable to CT states having largely triplet character and to their vibronic components.[7] Emission is dominated by a closely spaced manifold of at least three of the latter states.[4] At the temperatures

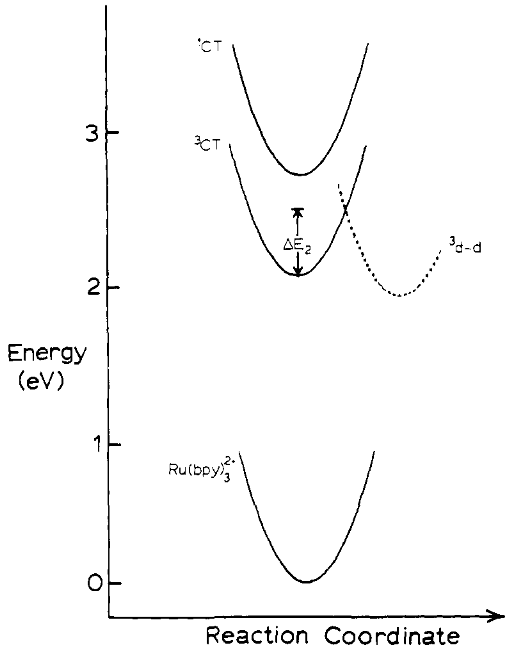

Figure 5. Potential energy diagram showing the ^1CT, ^3CT, and d-d excited states for $Ru(bpy)_3^{2+}$ in dichloromethane. The relative position of the ^3d-d state is unknown.

used in our experiments, the Boltzmann factors relating the three states are such (note ref 4 and the Results section) that emission from them is essentially temperature independent and can be viewed as occurring from a single state which we will label for convenience as ^3CT. However, the use of pure spin labels is an oversimplification. Many of the features of the absorption and emission spectra including absorption band energies and intensities can be satisfactorily accounted for by a recently developed theoretical model which assumes D_3 symmetry and incorporates spin-orbit coupling for the d^5 Ru(III) core.[20] The effect of spin-orbit coupling is to mix singlet character into the "triplet" states and vice versa, but the lowest lying states responsible for emission remain largely triplet in character. The efficiency of population of ^3CT following light absorption throughout the very-near-UV and visible spectral regions is known to be ~1.[21]

It seems unlikely that the origin of the photochemistry is in a CT excited state given the electronic structure expected for such a state, $(bpy)_2Ru^{III}(bpy^{-}\cdot)^{2+}$, and the known inertness to substitution of complexes of Ru(III). For example, complexes like $Ru(bpy)_2Cl_2^+$ and $Ru(bpy)_2(py)Cl^{2+}$ which have associated Ru(III)/Ru(II) reduction potentials (0.31 and 0.79 V in CH_3CN) near the excited-state $Ru(bpy_3)^{2+*}/Ru(bpy_3)^+$ potential (0.8 V)[9a] are stable indefinitely in water and in polar organic solvents. It is certainly clear from the absorption and emission data in Figure 1 and Table I that the spectroscopically observable excited states are relatively unaffected by those changes in medium which cause a change from relatively efficient photosubstitution (CH_2Cl_2, X^- = NCS^-) to no, or inefficient, photosubstitution (CH_2Cl_2, X^- = PF_6^-; acidic aqueous solution).

From the data in Table II and the earlier work of Allsop et al.,[19] kinetic decay parameters for ^3CT are medium dependent. From the data in Table II, radiative decay, k_r, is increased slightly in comparing water with dichloromethane while nonradiative decay, k_{nr}, is slower in CH_2Cl_2 by a factor of 2.8. These and related medium effects will be discussed in detail in a later publication.

Rather than the CT states, photosubstitution in $Ru(bpy)_3^{2+}$ appears to occur via a nonspectroscopically observable d-d state or states. As suggested by Van Houten and Watts,[11] the photochemical reaction is initiated by thermal activation to an upper, presumably d-d state[22-24] following population of ^3CT. From available evidence it is expected that ^3CT and the ground state are probably closely related structurally, at least in terms of the Ru-N coordination environment.[8,9,25] For a d-d excited state, an antibonding, metal-based orbital of e symmetry is occupied which is expected to lead to significant distortions along the Ru-N bonding axes.[26] An attempt is made in Figure 5 to show schematically the large distortions expected between the ^3CT and d-d excited states.

Scheme I

$$Ru(bpy)_3{}^{2+} \xrightarrow{h\nu} Ru(bpy)_3{}^{2+*} \xrightarrow[\phi\sim 1]{} {}^3CT$$

$$^3CT \xrightarrow{k_1} Ru(bpy)_3{}^{2+} \quad (k_1 = k_r + k_{nr})$$

$$^3C \underset{k_{-2}}{\overset{k_2}{\rightleftharpoons}} \text{d-d}$$

$$\text{d-d} \xrightarrow{k_3} \text{photoproducts}$$

$$\text{d-d} \xrightarrow{k_4} Ru(bpy)_3{}^{2+}$$

The importance of thermal activation to the d-d state is obvious from the experimental data. From the data in Figure 4 for substitution of NCS^- for 2,2'-bipyridine in CH_2Cl_2, ϕ_p decreases from 0.14 at 30 °C to ~0.005 at −20 °C where >90% of excited-state decay occurs via ^3CT ($k_r + k_{nr}$). There is good evidence from the work of Malouf and Ford[27] and of Figard and Petersen[28] that thermally equilibrated d-d and CT states can occur in the same energy region in related complexes.

Lifetime Measurements. Photochemical Mechanism. The discussion above suggests a photochemical mechanism consisting of the relatively simple sequence of reactions shown in Scheme I. Interpretation of the lifetime data in Table II using Scheme I leads to the following conclusions about the photochemical and photophysical properties of $Ru(bpy)_3^{2+}$ and related complexes.

1. $\Delta E'$ refers to the $^3CT \rightarrow$ d-d transition. Numerically, it is the same within experimental error in CH_2Cl_2 (PF_6^- salt) or in water. The differences in lifetime between water and dichloromethane are slight. At 25 °C, ~20% of the excited-state energy initially in ^3CT is dissipated through d-d while in dichloromethane the percentage is ~70%.

2. Values of k, k^0, and $\Delta E'$ in dichloromethane under photochemical (NCS^- salt) and nonphotochemical (PF_6^- salt) conditions are also identical within experimental error. The key steps in photosubstitution must occur at some stage following population of the d-d state.

3. The same overall pattern of kinetic parameters is maintained in the closely related complexes $Ru(bpy)_2(py)_2^{2+}$ and $Ru(phen)_3^{2+}$. In dichloromethane at 25 °C, the percentages of energy dissipated through the d-d state are ~56% for $Ru(bpy)_2(py)_2^{2+}$ and, remarkably, ~98% for $Ru(phen)_3^{2+}$. The close similarity in excited-state lifetimes between $Ru(bpy)_3^{2+}$ and $Ru(bpy)_2(py)_2^{2+}$ is especially striking given the remarkable differences in photosubstitution and luminescence quantum yields [$\phi_r(Ru(bpy)_2(py)_2^{2+}) \sim 10^{-2}\phi_r(Ru(bpy)_3^{2+})$] between the two ions. Once again, the origin of such differences is not in the dynamics of the $^3CT \rightarrow$ d-d transition given the similarity of the two ions with regard to the term $k^0 \exp(-\Delta E'/RT)$.

4. Returning to the quantum yield data in Table III, the decrease in ϕ_p in the presence of O_2 is expected given the well-

---

[20] Kober, E. R.; Meyer, T. J. *Inorg. Chem.*, in press.

[21] Demas, J. N.; Taylor, D. G. *Inorg. Chem.* **1979**, *18*, 3177.

[22] (a) Zinato, E. In "Concepts of Inorganic Photochemistry"; Adamson, A. W., Fleischauer, P. D. Eds.; Wiley-Interscience: New York, 1975; Chapter 4. (b) Ford, P. C.; Hintze, R. E.; Petersen, J. D. *Ibid.*, Chapter 5.

[23] Balzani, V.; Carasitti, V. "Photochemistry of Coordination Compounds"; Academic Press: New York, 1975.

[24] Vanquickenborne, L. G.; Ceulemans, A. *Inorg. Chem.* **1978**, *17*, 2730.

[25] Bock, C. R.; Connor, J. A.; Gutierrez, A. R.; Meyer, T. J.; Whitten, D. G.; Sullivan, B. P.; Nagle, J. K. *J. Am. Chem. Soc.* **1979**, *101*, 4815.

[26] (a) Wilson, R. B.; Solomon, E. I. *J. Am. Chem. Soc.* **1980**, *102*, 4085. (b) Miskowski, V. M.; Gray, H. B.; Wilson, R. B.; Solomon, E. I. *Inorg. Chem.* **1979**, *18*, 1410.

[27] Malouf, G.; Ford, P. C. *J. Am. Chem. Soc.* **1977**, *99*, 7213.

[28] Figard, J. E.; Petersen, J. D. *Inorg. Chem.* **1978**, *17*, 1059.

Scheme II

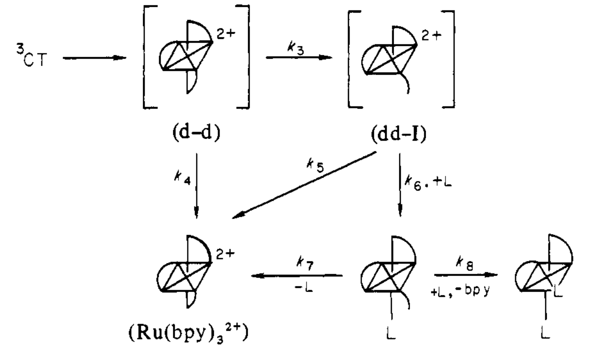

documented quenching of ^{3}CT by O_2.[29] The origin of the effect on ϕ_p is in a lowered efficiency for the ^{3}CT → d–d transition because of competitive bimolecular quenching by O_2. Under these conditions the lifetime expression is as shown in eq 10, $k' = k'^0 \exp(-\Delta E'/RT)$.

$$\tau^{-1} = k + k' + k_{O_2}(O_2) \tag{10}$$

It is doubtful that nonradiative or radiative decay of higher CT states having largely singlet character are important contributors to the exponential term, $k'^0 \exp(-\Delta E'/RT)$, in eq 2. Including an estimate for vibrational distortions,[25] the lowest energy gap between ^{1}CT and ^{3}CT states from absorption and emission data is ~4000 cm^{-1} which is appreciably larger than $\Delta E'$. From the results of Demas and Taylor,[21] $\phi \sim 1$ for ^{1}CT → ^{3}CT. From their result, even if ^{1}CT is populated thermally and decays rapidly to the ground state, the per event efficiency for such a pathway is necessarily considerably less than 1.

Quantum Yield Measurements. Photochemical Mechanism. Experimental insight into the reacting photochemical system is carried one step further by the photochemical quantum yield results presented here in dichloromethane and earlier in water by Van Houten and Watts.[11] In Scheme II is shown a mechanism, consistent with the experimental facts, which describes the fate of the d–d excited state once formed. Additional intermediates can be invoked, but the pattern of reactions in Scheme II is the simplest necessary to explain the photochemistry.

The justification for Scheme II is based on the following considerations. (1) Substitution appears to occur from the d–d state by a thermally activated dissociative (D or S_N1) mechanism which is not surprising since dissociative photochemistry is expected for strong-field d^6 cases.[30,31] This suggestion is supported by the absence of an entering group dependence in CH_2Cl for photosubstitution of X^- ($X^- = Cl^-, NCS^-, NO_3^-$) for py in $Ru(bpy)_2(py)_2^{2+}$.[15] The absence of an entering group dependence suggests capture of a completely formed five-coordinate intermediate with no memory effects from the lost pyridyl group (eq 11).

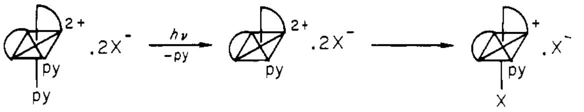 (11)

The entering group dependences for salts of $Ru(bpy)_3^{2+}$ or $Ru(phen)_3^{2+}$ (Table III) are understandable since now the dissociated pyridyl "leaving group" is held in the vicinity of the vacant coordination site (eq 12).

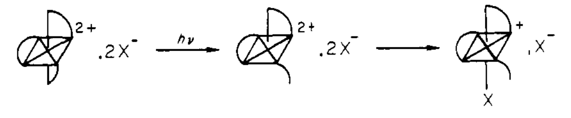 (12)

(2) Dissociation of the d–d state probably gives a five-coordinate intermediate (dd-I) which is square pyramidal in structure as might have been predicted.[24,30,31] If a trigonal bipyramid were formed it would lead to racemization of optically resolved $Ru(bpy)_3^{2+}$ because of the achiral nature of the intermediate. Photoracemization of $Ru(bpy)_3^{2+}$ in water has been observed,[32] but the racemization yield at 25 °C ($\phi = 2.9 \times 10^{-4}$) is considerably lower than the yield for formation of the d–d state under comparable conditions ($\phi = 0.04$; note below). Racemization can occur by a rearrangement through a trigonal-bipyramidal intermediate (eq 13). Presumably, racemization efficiency of the intermediate is less than one because the rearrangement process is in competition with the intermediate decay processes shown in Scheme II and the intermediate is not fully stereolabile.

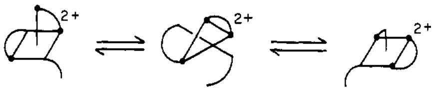 (13)

(3) There may be different intermediates for thermal and photochemical substitution. Photolysis of the related complex *cis*-$Ru(bpy)_2(H_2O)_2^{2+}$ leads to a trans rich cis/trans mixture,[16] while thermal substitution occurs with retention of the cis configuration. The difference could arise because of different electronic structures for the intermediates if both mechanisms are dissociative, or because different substitutional pathways are involved.

(4) There is direct evidence for the six-coordinate, unidentate bpy intermediate in Scheme II obtained by photolysis of the salt $[Ru(bpy)_3](NCS)_2$ in CH_2Cl_2.[15] However, the suggestion by Van Houten and Watts that the product of photolysis of $Ru(bpy)_3^{2+}$ in water is a stable, monodentate bpy complex appears to be incorrect. An analysis of their spectral results leads us to conclude that the initial photoproducts in their photolyses in Cl$^-$ media are $Ru(bpy)_2(H_2O)Cl^+$, $Ru(bpy)_2Cl_2$, and *cis*- and *trans*- $Ru(bpy)_2(H_2O)_2^{2+}$.[16] The spectral properties that they report can be reproduced by dissolving the carbonato complex, $(bpy)_2Ru(CO_3)$, in dilute acid and adjusting the Cl$^-$ concentration.

Interpretation of Rate Constant and Quantum Yield Values. In interpreting the experimental rate constant and quantum yield data, it is convenient to consider first the formation of the reactive d–d state and then its subsequent chemical and physical processes. Using the rate constants defined in Scheme I and the steady-state approximation for ^{3}CT leads to the expression in eq 14 for the

$$\frac{1}{\tau_0} = k_1 + k_2\left(\frac{k_3 + k_4}{k_{-2} + k_3 + k_4}\right) \tag{14}$$

lifetime of the emitting CT state. The constants in eq 14 are related to the experimental parameters k and k' by

$$k = k_1 = k_r + k_{nr}$$

$$k' = k_2\left(\frac{k_3 + k_4}{k_{-2} + k_3 + k_4}\right) = k'^0 \exp(-\Delta E'/RT) \tag{15}$$

Equation 15 has two limiting forms. In the first, $k_{-2} >> (k_3 + k_4)$, which leads to eq 16. In this limit the d–d state is in

$$k' = (k_3 + k_4)(k_2/k_{-2}) = k'^0 \exp(-\Delta E'/RT) \tag{16}$$

equilibrium with ^{3}CT and undergoes further reaction (k_3) or decays to the ground state (k_4). If the limiting case described by eq 16 is valid, the experimental constants k'^0 or $\Delta E'$ are complex and cannot by interpreted unambiguously. However, it is probably safe to assume that the exponential term is dominated by the energy gap between the d–d and ^{3}CT states.

In the second limiting form of eq 15, $k_{-2} << (k_3 + k_4)$ which gives eq 17. In this limit the ^{3}CT → d–d transition becomes an

$$1/\tau_0 = k_1 + k_2 = k_1 + k_2^0 \exp(-E_{a,2}/RT) \tag{17}$$

irreversible surface crossing having an energy of activation $E_{a,2}$ and a preexponential factor k_2^0. If this limit is appropriate, the

---

[29] Demas, J. N.; Harris, E. W.; McBride, R. P. *J. Am. Chem. Soc.* **1977**, *99*, 3547. Demas, J. N.; Harris, E. W.; Flynn, C. M., Jr.; Diemente, D. *Ibid.* **1975**, *97*, 3838.

[30] Clark, S. F.; Petersen, J. D. *Inorg. Chem.* **1979**, *18*, 1818, 3394.

[31] Skibsted, L. H.; Strauss, D.; Ford, P. C. *Inorg. Chem.* **1979**, *18*, 3171.

[32] Porter, G. B.; Sparks, R. H. *J. Photochem.* **1980**, *13*, 123.

Table IV. Photochemical Parameters at 25 °C[a]

complex	medium	$10^6\tau_0$, s	$10^{-6}k'$, s^{-1}	ϕ_p	ϕ_l	ϕ_p(d–d)
Ru(bpy)$_2$(py)$_2^{2+}$	CH$_2$Cl$_2$(NCS$^-$)[b]	0.50	1.1	~0.3[c]	0.55	~0.5
	H$_2$O			~0.3		
Ru(bpy)$_3^{2+}$	CH$_2$Cl$_2$(NCS$^-$)	0.52	1.1	0.068	0.57	0.086
	H$_2$O(0.1*M* HCl)	0.58	0.36	0.000021	0.21	0.00011[d]
Ru(phen)$_3^{2+}$	CH$_2$Cl$_2$(NCS$^-$)[b]	0.15	6.2	0.020	0.98	0.020

[a] The various parameters are defined in the text. [b] The PF$_6^-$ salt was used for lifetime measurements and the NCS$^-$ salt for photosubstitution quantum yields. [c] Note ref 33. [d] Calculated from lifetime and quantum yield data taken from ref 11.

experimental and mechanistic rate constants are related straightforwardly:

$$k = k_1$$

$$k' = k'^0 \exp(-\Delta E'/RT) = k_2{}^0 \exp(-E_{\mathrm{a},2}/RT) \qquad (18)$$

Consider next the chemical and physical processes of the d–d state. The experimental quantum yield for substitution (ϕ_p) can be written as the product of the quantum yield for the ^{3}CT → d–d transition (ϕ_i) and the intrinsic quantum yield for substitution once the d–d state has been reached (ϕ_p(d–d)) (eq 19). The

$$\phi_\mathrm{p} = \phi_\mathrm{i}\phi_\mathrm{p}(\text{d–d}) \qquad (19)$$

quantum yield, ϕ_i, is defined in terms of the constants in Scheme I by eq 20

$$\phi_\mathrm{i} = k_2/(k_1 + k_2) \qquad (20)$$

if it is assumed for simplicity that the surface crossing limit is appropriate.

The most useful comparisons of the innate photochemical reactivity are those in which the efficiency of reaction following population of the d–d state is used. This quantity, ϕ_p(d–d), is a direct measure of the substitutional characteristics of the d–d excited state. In terms of experimentally measured parameters, ϕ_p(d–d) is given by eq 21. Values for ϕ_p(d–d) and the parameters

$$\phi_\mathrm{p}(\text{d–d}) = \frac{\phi_\mathrm{p}}{\phi_\mathrm{i}} = \frac{\phi_\mathrm{p}}{\tau_0 k'^0 \exp(-\Delta E'/RT)} \qquad (21)$$

needed to calculate it are collected for the three complexes of interest in Table IV.

From Table IV, ϕ_p(d–d) ~ 0.5 at 25 °C for the salt [Ru(bpy)$_2$(py)$_2$](NCS)$_2$ in CH$_2$Cl$_2$. The magnitude of the value shows that, once populated, the d–d state is *highly* reactive toward loss of pyridine. We have no way of knowing whether opening of a chelate ring (eq 22) also occurs. The process may occur but cannot

$$\underset{(\text{d–d})}{(\text{bpy})(\text{py})_2\text{Ru}(\text{bpy})^{2+*}} \rightarrow (\text{bpy})_2(\text{py})_2\text{Rupy–py}^{2+} \qquad (22)$$

be of great importance compared with loss of pyridine. No evidence has been found for bpy-loss photoproducts, even in CH$_2$Cl$_2$ where efficient trapping of the intermediate would be expected to occur.

$$[(\text{bpy})_2(\text{py})_2\text{Ru}(\text{py}{\sim}\text{py})^{2+}],\ 2\text{X}^- \rightarrow [(\text{bpy})_2(\text{py})_2\text{Ru}(\text{py–py})\text{X}^+]\text{X}^- \qquad (23)$$

For the tris-chelate salts, [Ru(bpy)$_3$](NCS)$_2$ or [Ru(phen)$_3$](NCS)$_2$ in CH$_2$Cl$_2$, the photosubstitutional reactivity of the d–d state at 25 °C falls; ϕ_p(d–d) = 0.086 and 0.020, respectively. The decreases in reactivity are not profound and can be accommodated by the mechanism in Scheme II. Defining ϕ_p(d–d) in terms of the constants in Scheme II gives

$$\phi_\mathrm{p}(\text{d–d}) = \left(\frac{k_3}{k_3 + k_4}\right)\left(\frac{k_6}{k_5 + k_6}\right)\left(\frac{k_8}{k_7 + k_8}\right) = \frac{k_3F}{k_3 + k_4} \qquad (24)$$

$$F = F_1F_2 = \left(\frac{k_6}{k_5 + k_6}\right)\left(\frac{k_8}{k_7 + k_8}\right)$$

Equation 24 includes the effects of chelate ring closure to give Ru(bpy)$_3^{2+}$ both from the five-coordinate intermediate (F_1) and from the unidentate, six-coordinate intermediate (F_2). The fall in ϕ_p(d–d) for the tris chelates could be due to decreases in either or both F_1 and F_2. It should be noted that in CH$_2$Cl$_2$, F_2 is necessarily 1 for both Ru(bpy)$_3^{2+}$ and Ru(bpy)$_2$(py)$_2^{2+}$. For Ru(bpy)$_2$(py)$_2^{2+}$, Ru(bpy)$_2$(py)NCS$^+$ is a stable product and for Ru(bpy)$_3^{2+}$ spectral studies have shown that the intermediate (bpy)$_2$(NCS)Ru(py-py)$^+$ undergoes an additional thermal reaction to give Ru(bpy)$_2$(NCS)$_2$ exclusively.[15]

The temperature dependence of ϕ_p(d–d) for [Ru(bpy)$_3$](NCS)$_2$ in CH$_2$Cl$_2$ can be determined from eq 19 and the temperature dependences of ϕ_p. The form of the experimental temperature dependence for ϕ_p was given in eq 9, and from eq 9 and 19 the temperature dependence for ϕ_p(d–d) is given by eq 25. Using

$$\phi_\mathrm{p}(\text{d–d}) = \frac{\phi_\mathrm{p}}{\phi_\mathrm{i}} = \frac{a \exp(-\Delta E''/RT)}{b + a \exp(-\Delta E''/RT)} \qquad (25)$$

a least-squares fitting routine gave for the parameters in eq 25, a/b = 667 and $\Delta E''$ = 1870 cm^{-1}.

The form of eq 25 is kinetically consistent with eq 24 under certain conditions; e.g., $a/b = (k_3/k_4)(\exp(-\Delta E''/RT)^{-1} = 667$ and F = 1. However, it should be appreciated that, because of the limited amount of data, it is not possible to define the kinetic parameters with certainty. The real value of the fitting procedure is in establishing the form of the temperature dependence to show that it is consistent with the predictions of Scheme II. Once again, an unambiguous interpretation of the exponential terms containing $\Delta E''$ is not possible because of the complexity of the mechanism. However, it is not unreasonable to suggest that an important contribution to $\Delta E''$ comes from thermal activation of the d–d state in the bond-breaking step, d–d → dd-I.

Possible origins for the photochemical solvent effect between CH$_2$Cl and H$_2$O can also be explained using the mechanism in Scheme II. The effect does not exist for Ru(bpy)$_2$(py)$_2^{2+}$ where efficient photochemistry occurs in either solvent. For Ru(bpy)$_3^{2+}$, the major effect of the solvent must occur past the ^{3}CT → d–d transition. From Table IV, ϕ_i differs by a factor of less than 3 between solvents at 25 °C while the difference in ϕ_p(d–d) is ~800.

Van Houten and Watts have published the temperature dependence of ϕ_p and ϕ_i for Ru(bpy)$_3^{2+}$ in water.[11] Using our fitting procedure and their data we obtain $\Delta E''$ ~ 2000 cm^{-1}. The similarity in $\Delta E''$ values for Ru(bpy)$_3^{2+}$ in the two solvents (1870 vs. 2000 cm^{-1}) and the lack of solvent dependence for Ru(bpy)$_2$(py)$_2^{2+}$ are both striking observations. They point strongly to a primary origin for the solvent effect that is even past the thermally activated d–d → dd-I bond-breaking step. From Scheme II and eq 24, the remaining steps where solvent could play a major role involve either of two possibilities: (1) the lower coordinate intermediate dd-I where a competition exists between chelate ring closure and capture by L [($F_1 = k_6/(k_5 + k_6)$] or (2) the six-coordinate, unidentate intermediate (bpy)$_2$(L)Ru$^{\mathrm{II}}$(py–py) where there is a competition between chelate ring closure to give Ru(bpy)$_3^{2+}$ and loss of bpy to give (bpy)$_2$Ru$^{\mathrm{II}}$L$_2$ [($F_2 = k_8/(k_7 + k_8)$)].

A significant solvent effect is expected for F_2. In 1 M aqueous pyridine at room temperature, the reaction, Ru(bpy)$_2$(py)H$_2$O^{2+} + py → Ru(bpy)$_2$(py)$_2^{2+}$ + H$_2$O, occurs with a halftime of ~7.2 min. Given the expected kinetic advantages of chelate ring closure over bimolecular substitution, the reaction (bpy)$_2$(H$_2$O)Ru(py–py)$^{2+}$ → Ru(bpy)$_3^{2+}$ + H$_2$O is expected to be considerably faster and favored thermodynamically. In CH$_2$Cl$_2$ the situation is reversed. Equilibria like

$$X^- + Ru(bpy)_2(py)_2^{2+} \rightleftarrows Ru(bpy)_2(py)X^+ + py$$

lie to the right. An important factor determining the position of equilibrium is the loss in solvation energies for $Ru(bpy)_2(py)_2^{2+}$ and especially X^- between water ($D_s = 78.5$) and dichloromethane ($D_s = 8.9$). For an intermediate like [(bpy)$_2$Ru(NCS)bpy]NCS in dichloromethane, chelate ring formation may well be disfavored thermodynamically and, in addition, the monodentate bpy ligand could well become an objectionable group sterically and be prone to thermal dissociation.

If the majority of the solvent effects are in the reactivity of the six-coordinate, unidentate intermediate, a novel conclusion is reached. $Ru(bpy)_3^{2+}$ *is inherently photochemically reactive* in both solvents. The major difference in photochemical behavior is that for the intermediate $(bpy)_2(L)Ru^{II}(py\text{–}py)$, chelate ring closure is favored in water where $L = H_2O$, and bpy loss is favored in CH_2Cl_2 where $L = X^-$.

Conclusions

A number of important conclusions can now be drawn about the photochemistry of $Ru(bpy)_3^{2+}$.

(1) At ambient temperatures and above, $Ru(bpy)_3^{2+}$ is, in an intrinsic sense, relatively reactive photochemically.

(2) A major contribution to the apparent photochemical solvent effect between water and dichloromethane appears to be in the thermodynamic preferences of a six-coordinate intermediate relatively far removed from the critical photochemical steps. The apparent photochemical stability of $Ru(bpy)_3^{2+}$ in water compared to $Ru(bpy)_2(py)_2^{2+}$ is a consequence of a "self-annealing" protective step, chelate ring closure.

(3) In catalytic photoredox applications, photochemical substitution can be suppressed by the addition of sufficient quencher to capture ^{3}CT before surface crossing to ^{3}d–d can occur. The extent of photodegradation per cycle will depend on ϕ_i and ϕ_p(d–d) in the medium, the temperature, and the percentage of ^{3}CT quenched by the added quencher. If our results are translatable to other media, photochemical degradation can be minimized by considering the following: (a) potentially coordinating anions in solvents of low dielectric constant should be avoided;[15] (b) stability can be enhanced by having sufficiently high quencher concentrations to achieve nearly complete quenching; (c) stability can also be enhanced by working at temperatures below ambient.

(4) At ambient temperature and above, an increasingly important percentage of ^{3}CT excited-state decay occurs via the d–d excited state.

(5) The intervention of the d–d state may appear in the results of other experiments. From a pulse radiolysis experiment, the product distribution for reduction of $Ru(bpy)_3^{3+}$ by e$^-$(aq) was ~7% $Ru(bpy)_3^{2+}$, 38% $Ru(bpy)_3^{2+}$ (^{3}CT) and 55% of an unknown intermediate which also "decays" to the ground state.[34] It is quite conceivable that the intermediate is $(bpy)_2(H_2O)Ru(py\text{-}py)^{2+}$ formed by the sequence of reactions, $Ru(bpy)_3^{3+} + e_{aq}^- \rightarrow Ru(bpy)_3^{2+}(d\text{–}d) \rightarrow (bpy)_2Ru(py\text{–}py)^{2+}(dd\text{-}I) \rightarrow (bpy)_2(H_2O)Ru(py\text{–}py)^{2+}$. In the sequence, the photochemical events are initiated by electron transfer to a dσ^*(Ru) orbital to give the d–d state rather than to a π^*(bpy) orbital, which would give ^{3}CT, or to a dπ orbital to give the ground state. The d–d state may also enter in a significant way into chemi- and electrochemiluminescence yields based on reduction of $Ru(bpy)_3^{3+}$.[35] The pulse radiolysis experiment raises the general possibility of observing charge-transfer-induced photosubstitution.

(6) Future studies on a series of related complexes should give insight into the factors determining the energetics for the ^{3}CT → d–d transition and possibly of the energy difference between the thermally equilibrated ^{3}CT and d–d states. From these and related experiments it may prove possible in a systematic way to understand in detail the microscopic origins of excited-state lifetimes in these and related complexes.

Acknowledgments are made to the Chaim Weizmann Postdoctorate Fellowship Program for fellowship support for B. Durham, to the National Science Foundation under Contract No. CHE8008922 for support of this research, and to Ed Kober and Peter Wagner for helpful discussions.

Registry No. $[Ru(bpy)_3](PF_6)_2$, 60804-74-2; $[Ru(bpy)_3](ClO_4)_2$, 15635-95-7; $[Ru(bpy)_3](SCN)_2$, 72525-88-3; $[Ru(bpy)_3](B(C_6H_5)_4)_2$, 50584-04-8; $[Ru(bpy)_2(py)_2](PF_6)_2$, 71230-35-8; $[Ru(phen)_3](PF_6)_2$, 60804-75-3; $[Ru(bpy)_3]Cl_2$, 14323-06-9; $[Ru(bpy)_3]Br_2$, 15388-41-7; $[Ru(phen)_3](NCS)_2$, 52501-85-6; $[Ru(phen)_3]Cl_2$, 23570-43-6; $[Ru(bpy)_2(py)_2](NCS)_2$, 82338-60-1; $Ru(bpy)_3^{2+}$, 15158-62-0.

---

(33) The quantum yield values for $[Ru(bpy)_2(py)_2]X_2$ in CH_2Cl_2, $\phi_p = 0.18$, refer to aerated solutions.[15] Assuming the same quenching rate constant by O_2 for $Ru(bpy)_3^{2+}$ (^{3}CT) and $Ru(bpy)_2(py)_2^{2+}$ (^{3}CT), and noting that the lifetimes for the two excited states are essentially the same at 25 °C (Table II) gives $\phi_p = 0.3$.

(34) Jonah, C. D.; Matheson, M. S.; Meisel, D. *J. Am. Chem. Soc.* **1978**, *100*, 1449.

(35) Tokel-Takvoryan, N. E.; Hemingway, R. E.; Bard, A. J. *J. Am. Chem. Soc.* **1973**, *95*, 6582. Itoh, K.; Honda, K. *Chem. Lett.* **1979**, *99*, 102.